Double quantum dots in suspended carbon nanotubes

Hüttel, AK; Witkamp, B; van der Zant, HSJ

DOI
10.1088/1742-6596/92/1/012037

Publication date
2007

Document Version
Final published version

Published in
Journal of Physics: Conference Series

Journal of Physics: Conference Series

Double quantum dots in suspended carbon nanotubes

To cite this article: A K Hüttel *et al* 2007 *J. Phys.: Conf. Ser.* **92** 012037

Double quantum dots in suspended carbon nanotubes

A K Hüttel, B Witkamp and H S J van der Zant

Molecular Electronics and Devices, Kavli Institute of Nanoscience Delft, Delft University of Technology, PO Box 5046, 2600 GA Delft, The Netherlands

E-mail: `mail@akhuettel.de`

Abstract. We present fabrication of and the first measurements on suspended double quantum dots in a carbon nanotube. When fabricating our devices, nanotubes grown on-chip are localized by AFM scanning, and subsequently contacted and gated with customized electrode geometries. Preliminary low-temperature transport measurement results are discussed, where the double quantum dot characteristics are clearly recognizable in measured current.

1. Motivation

In nano-electromechanical systems (NEMS) carbon nanotubes (CNT's) excel in many ways. Their high tensile strength and aspect ratio make them ideal as molecular mechanical resonators [1, 2]. Because of their low mass, CNT's show promise for approaching the quantum limit of mechanical motion. In addition, the extraordinary properties of carbon nanotubes as "one-dimensional molecular conductors" [3, 4] provide means of electronically accessing the mechanical properties in the quantum regime [5].

Previous experiments have shown [5] that longitudinal (stretching mode) vibronic excitations of CNT quantum dots can be resolved in transport measurements as sets of harmonic excited states at low energy. The transversal or bending mode can more directly couple to the electric field between quantum dot and back gate charges, so a larger electron–phonon coupling is expected. The direct observation of this mode − with a corresponding energy scale of $\hbar\omega \lesssim 30\,\mu\text{eV}$ at obtainable nanotube lengths $L \geq 90\,\text{nm}$ − in low-temperature transport measurements, however, provides a technological challenge.

One way to potentially increase the energy resolution in transport measurements is to use a double quantum dot (DQD) [6, 7] defined within the CNT as spectrometer. For a DQD with very weak tunnel coupling, the obtainable energy resolution can here be limited by the tunnel rates between the quantum dots and the leads alone, independent of the electron temperature of the leads [6]. Measurements on DQD devices may thus lead to further insights on the electron-phonon coupling in CNT NEMS.

2. Fabrication methods

The starting point of our fabrication is a bare SiO_2 on Si substrate with an oxide thickness of typically $0.5 - 1\,\mu\text{m}$. At first, e-beam and AFM alignment markers are defined lithographically. Typically, for the e-beam alignment markers, a metallization of 5 nm titanium (as adhesion layer) and 60 nm platinum provides good contrast. As the marker shape is critical, $30 - 50$ nm chromium is used for the AFM marker grid because of its high thermal stability during the CNT

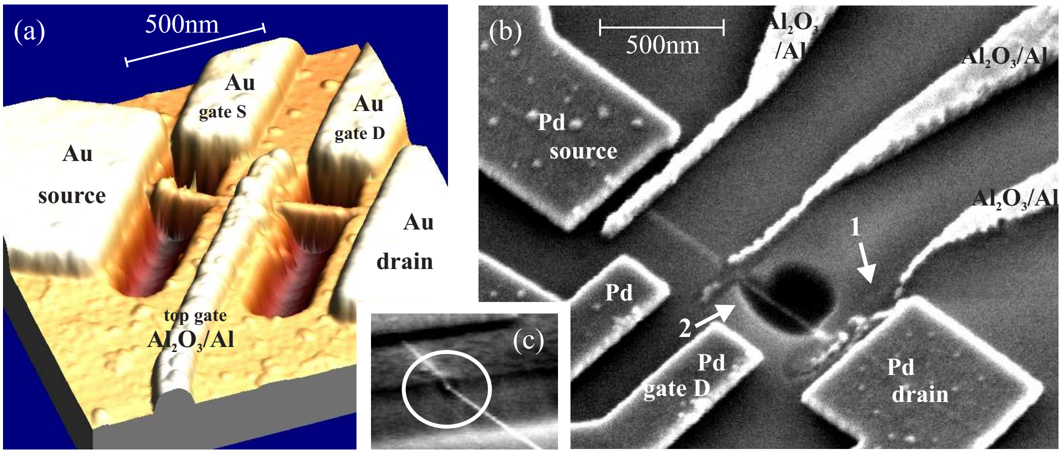

Figure 1. Device geometries: (a) AFM picture of a CNT double quantum dot structure (underetched on both sides), with Cr/Au leads and an Al_2O_3/Al/AuPd central top gate. (b) SEM micrograph of a device underetched only on one side, with Ti/Pd contacts and three Al_2O_3/Al/AuPd top gates. Typical fabrication difficulties are marked with arrows (see text). (c) Detail SEM micrograph, showing a CNT pulled into the etched hole by surface tension during drying (see text).

growth. Subsequently a further lithography step is used to locally deposit catalyst for in-situ chemical vapour deposition growth of CNT's [8].

The position of the resulting CNT's is determined by atomic force microscopy (AFM). The AFM scans are imported into a CAD system; script-driven CAD processing is used to "draw" device geometries with preselected dimensions (e.g. electrode width, separation between electrodes, ...) at the required coordinates. Subsequently, the electrodes are fabricated using electron beam lithography.

Figure 1 displays two different approaches to fabricating a (partially) suspended DQD. In the device in the AFM picture of Fig. 1(a), the CNT is contacted with leads formed by a chromium adhesion layer below gold. Since this layer structure typically leads to a highly resistive tunneling contact [9], it has been used previously to directly form a quantum dot between the contact electrodes [10]. This same effect is used here to define the tunnel barriers between the DQD and its leads. The central tunnel barrier between the two quantum dots of the DQD is generated by local gating of the electrochemical potential with an aluminum oxide / aluminum top gate electrode [11]. Figure 1(b) displays a device using a complementary approach for the electrode geometry. Here, the contacts are formed by palladium on top of a thin titanium adhesion layer, which in turn generally leads to a low-resistance (Ohmic) contact between metal and CNT [12]. As a consequence, three top gates (generating the tunnel barriers source – dot 1, dot 1 – dot 2, and dot 2 – drain, respectively) are required. This provides a high level of control over the potential landscape.

For both device geometry variants, suspending the CNT is done by wet underetching in ammonium fluoride etching mixture. Care must be taken that the aluminum oxide / aluminum top gates do not come into contact with the etchant. For this purpose, in a further lithographic step the electron beam lithography resist PMMA is used as etch mask [2].

3. First results

Figure 2 displays first measurements of partially functional structures. All data have been recorded in a dilution refrigerator setup at $T_{\mathrm{MC}} \lesssim 20\,\mathrm{mK}$ and $T_{\mathrm{el}} \sim 100\,\mathrm{mK}$. In Fig. 2(a) and

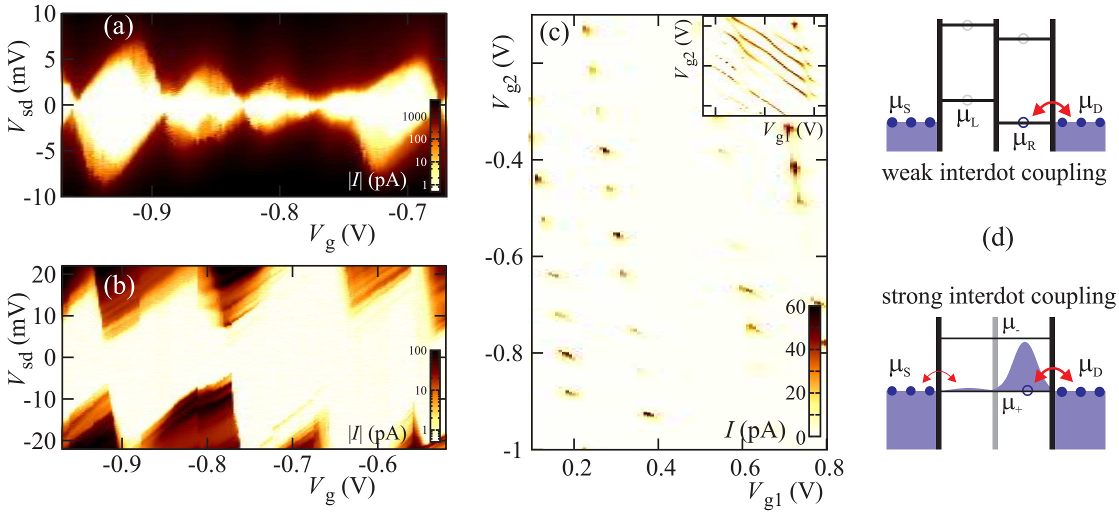

Figure 2. First measurements of partially functional devices: (a), (b): Absolute value of the dc current through a CNT DQD structure, as function of back gate voltage V_g and source-drain voltage V_{sd} for center top gate voltage (a) $V_{tg\text{-}c} = -1.2\,V$ and (b) $V_{tg\text{-}c} = +1.2\,V$. The gating effect towards a DQD potential structure for holes is recognizable. (c): dc-current through a CNT DQD with weak interdot coupling as function of the two side gate voltages for a finite source-drain voltage $V_{sd} = 200\,\mu V$. Insert: example of a similar measurement at strong interdot coupling. (d) Level schemata for tunneling through a DQD in these limiting cases.

(b), current through a DQD device is plotted as function of back gate voltage V_g and source-drain voltage V_{sd}. The central top gate voltage is chosen as (a) $V_{tg\text{-}c} = -1.2\,V$ and (b) $V_{tg\text{-}c} = +1.2\,V$. Whereas Fig. 2(a) displays nearly regular Coulomb blockade regions with a charging energy of up to 10 meV and broadened edges, in Fig. 2(b) a more than doubled charging energy of $\gtrsim 20\,meV$, a large, highly irregular region of suppressed current around zero bias ($|V_{sd}| \lesssim 5\,mV$) and sharp resonances of enhanced current at finite bias are observed. Comparing the two measurements, it becomes immediately clear that the nanotube is in the hole conduction regime and that in Fig. 2(b) for more positive gate voltage a central potential barrier is formed below the top gate. Misalignment of the chemical potentials in the two formed quantum dots leads to single electron tunneling suppression for a large bias region, alignment of ground and / or excited states to current maxima [6].

Figure 2(c) displays data taken from a different device. The dc current at $V_{sd} = 0.2\,mV$ is plotted as function of the applied voltage on the two side gates controlling the chemical potentials of the two quantum dots. In the parameter region shown, the characteristic stability diagram of a DQD at weak tunnel coupling and weak capacitive coupling can be immediately recognized [13]. At the triple points of the stability diagram where the electron number in both quantum dots can fluctuate [6, 7], discrete maxima of single electron tunneling current occur. Measurements at higher source-drain bias display the expected broadening of the triple points into triangular regions of finite current (data not shown).

As contrast, the insert of Fig. 2(c) displays an example for the case of strong interdot coupling, where current can flow via delocalized quantum states even if the levels of both quantum dots are detuned. This is also illustrated in the level schemes of Fig. 2(d) for the two limiting cases.

4. Challenges and outlook

DQD characteristics have been clearly observed in low-temperature transport measurements. Thus, there is a promising prospect of attaining a fully tunable weakly coupled DQD as spectrometer, and work on the respective chip structures is ongoing.

One important objective of our current work is improving the device fabrication yield. As can be observed in Fig. 1(b), the etch mask technique at the moment does not completely protect the aluminum oxide / aluminum top gates from the hydrofluoric acid (see e.g. arrow 1 in Fig. 1(b)). Improvements towards decreasing edge roughness of the metal and / or a better coverage during etch mask lithography are required, as well as research into alternative top gate and isolator materials. Judging from the shape of the etched holes, the etchant in addition flows along the CNT (see arrow 2).

Imaging the devices fabricated up to now, further potential challenges can be identified. Surface tension during the drying process can cause the CNT not to pass straight across the etched "hole". Instead the CNT follows the oxide surface for a small distance – bending into the hole – before stretching across the hole at a lower height. This is illustrated in the detail SEM micrograph of Fig. 1(c). Effectively, several kinks are introduced in the CNT, potentially leading to tension and local potential barrier structures. Currently tests using a critical point dryer are conducted in order to fully eliminate such surface tension effects.

Regarding the measurements, a common characteristic that has been observed several times in transport measurements has been a suppression of zero-bias current, as also shown in Fig. 2(a) (the "single-dot limit"). Although the observations are not fully conclusive up to now, it seems that this effect is also present in the DQD stability diagrams as e.g. Fig. 2(c), which rules out misalignment of the double quantum dot pseudo-potentials as a possible cause. Whether the suppression is caused by additional potential barriers, as e.g. at the aforementioned bends of the CNT or growth / fabrication defects, or by phonon blockade effects [14, 15] remains to be decided by additional measurements.

Acknowledgments
Many thanks go to the Dutch organization for Fundamental Research on Matter (FOM), the NWO VICI program, and to the EC CANEL project (contract no. FP6-2004-IST-003673) for financial support. This publication reflects the views of the authors and not necessarily those of the EC. The Community is not liable for any use that may be made of the information contained herein.

References

[1] Sazonova V, Yaish Y, Ustunel H, Roundy D, Arias T A and McEuen P L 2004 *Nature* **431** 284
[2] Witkamp B, Poot M and van der Zant H S J 2006 *Nano Letters* **6** 2904
[3] Oreg Y, Byczuk K and Halperin B I 2000 *Phys. Rev. Lett.* **85** 365
[4] Jarillo-Herrero P, Sapmaz S, Dekker C, Kouwenhoven L P and van der Zant H S J 2004 *Nature* **429** 389
[5] Sapmaz S, Jarillo-Herrero P, Blanter Y M, Dekker C and van der Zant H S J 2006 *Phys. Rev. Lett.* **96** 026801
[6] van der Wiel W G, De Franceschi S, Elzerman J M, Fujisawa T, Tarucha S and Kouwenhoven L P 2002 *Rev. Mod. Phys.* **75** 1
[7] Qin H, Holleitner A W, Hüttel A K, Blick R H, Wegscheider W, Bichler M, Eberl K and Kotthaus J P 2004 *phys. stat. sol. (c)* **1** 2094
[8] Kong J, Soh H T, Cassell A M, Quate C F and Dai H 1998 *Nature* **395** 878
[9] Bockrath M, Cobden D H, McEuen P L, Chopra N G, Zettl A, Thess A and Smalley R E 1997 *Science* **275** 1922
[10] Sapmaz S, Jarillo-Herrero P, Kouwenhoven L P and van der Zant H S J 2006 *Semic. Sci. Techn.* **21** S52
[11] Sapmaz S, Meyer C, Beliczynski P, Jarillo-Herrero P and Kouwenhoven L P 2006 *Nano Letters* **6** 1350
[12] Javey A, Guo J, Wang Q, Lundstrom M and Dai H 2003 *Nature* **424** 654
[13] Hofmann F, Heinzel T, Wharam D A, Kotthaus J P, Böhm G, Klein W, Tränkle G and Weimann G 1995 *Phys. Rev. B* **51** 13872
[14] Braig S and Flensberg K 2003 *Phys. Rev. B* **68** 205324
[15] Weig E M, Blick R H, Brandes T, Kirschbaum J, Wegscheider W, Bichler M and Kotthaus J P 2004 *Phys. Rev. Lett.* **92** 046804